

Electrocapillarity of an electrolyte solution in a nanoslit with overlapped electric double layer: Continuum approach

Jung A. Lee and In Seok Kang*

Department of Chemical Engineering, Pohang University of Science and Technology, San 31, Hyoja-dong, Pohang 790-784, South Korea

(Received 25 April 2013; revised manuscript received 23 March 2014; published 3 September 2014)

A nanoslit is a long narrow opening between two parallel plates that are nanometers apart from each other. When an electrolyte solution is present inside a nanoslit, an overlapped electrical double layer (EDL) is formed and there exist distributions of the osmotic pressure and the Maxwell stress across the nanoslit. It is well known that the total normal stress (osmotic pressure contribution + Maxwell stress contribution) in the direction normal to the nanoslit surface is uniform and the value is the same as the osmotic pressure at the centerline. On the other hand, it is not well known that the total normal stress in the direction parallel to the slit surface is not uniform. When there is an electrolyte-gas interface inside a nanoslit, this total normal stress in the direction parallel to the slit surface generates the electrocapillarity effect. In the present work, the electromechanical approach is adopted to estimate the electrocapillarity effect in terms of the slit surface potential (or the surface charge density), the gap size, and the bulk ion concentrations. In order to handle the problem analytically, it is assumed that the nanoslit problem is in the continuum range and the interface is initially flat. The deformation of the interface due to the nonuniform total normal stress along the interface is also obtained by using the first order perturbation method. The significance of the present work can be manifested by the fact that external voltage is frequently used in nanoscaled systems and the electrocapillarity effect should be considered in addition to the intrinsic capillarity due to surface tension.

DOI: [10.1103/PhysRevE.90.032401](https://doi.org/10.1103/PhysRevE.90.032401)

PACS number(s): 68.03.-g, 47.55.nb

I. INTRODUCTION

When an electrode is immersed in an electrolyte solution, the attracted counterions push each other to exhibit collectively the electrocapillarity phenomenon. If there is a thin dielectric layer between the electrolyte solution and the electrode, external voltage can be applied and significant change of the (apparent) contact angle can be achieved. This kind of contact angle change is called electrowetting on a dielectric or in short, electrowetting [1].

Electrowetting has been regarded as a very efficient tool for the handling of microfluids [1–5]. Indeed it has been applied in various areas such as actuation of microfluids and optomicrofluidics [6,7]. The availability of a high quality thin dielectric layer enables low-voltage electrowetting and even more promising applications are now possible [8]. The principle of electrowetting has also been applied in a reverse way. A noble mechanical-to-energy conversion method was proposed based on the reverse electrowetting phenomenon [9].

Theories on the electrowetting phenomenon started with the well-known Lippmann equation which predicts the (apparent) contact angle change as a function of voltage [10]. The Lippmann equation is based on the assumption that the drop is perfectly conducting as mercury. So, there have been several efforts to extend the theory for more general situations. In this direction, there are basically two approaches: the free-energy-based approach and the electromechanical approach. Buehrle *et al.* [11] used free-energy formulation to extend the theory to an electrolyte system. Biesheuvel [12] obtained electrostatic free energy considering chemical work as well as electrical work. On the other hand, Jones

[13] and Kang [14] showed that the Lippmann equation can be derived by the electromechanical approach. Then Kang *et al.* [15] applied the same approach to extend the theory for the aqueous electrolyte system, which has finite thickness of electrical double layer (EDL). The theory has been further extended to include the steric effects of ions in the electrolyte solution [16,17]. The electromechanical approach has also been adopted for computation of the wetting tension in ac electrowetting [18,19].

Recently, the interest in the electrowetting and electrocapillarity phenomena has been expanded down to the nanoscale and there have been considerable works. Because of the size of the problem, most of them are for the electrocapillarity effect. Research on the nanoscale electrocapillarity phenomenon can be categorized into two groups according to the nanotube diameter [20]: (i) a nanotube of diameter less than 10 nm, and (ii) a nanotube of diameter equal to or greater than 10 nm. The first category problems have been studied quite actively in order to see the noncontinuum behaviors [21,22]. These problems have been analyzed mostly by the molecular dynamics simulation to understand the wetting phenomena in a subnanometer scale such as in a carbon nanotube [23]. One important finding is that there may exist a water-depleted layer between water and the hydrophobic nanoscale surface because of hydrogen bonding [22].

In the second category problems of $O(10\text{ nm})$, the EDL is expected to be overlapped, but noncontinuum behaviors are not necessarily expected. These problems have been studied experimentally with some applications in mind (e.g., development of smart material), where a considerable amount of volume of liquid is to be handled [24,25]. They measured the extra pressure that is needed to be applied to the external fluid in order to make a balance to the electrowetting or electrocapillarity effect in a nanotube. However, interpretation of their results has been based on the classical Lippmann

*Author to whom correspondence should be addressed: iskang@postech.ac.kr

equation due to the lack of appropriate theories. Indeed, differently from the noncontinuum range problems, systematic analysis has not been performed on the problems in the continuum range of $O(10 \text{ nm})$ scale.

When the EDL is overlapped in an electrowetting or electrocapillarity problem, several things are different from the conventional macroscale counterpart [26–29]. First, coions are reduced within the nanotube or nanoslit even at the centerline. In other words, the coion concentration is smaller than the bulk value. Secondly, the electrical stress is not concentrated near the triple contact line (TCL), but it is distributed over the whole interface to result in some smooth distribution. In the case of macroscale electrowetting, the concentrated electrical stress near TCL results in the change of apparent contact angle [16,30]. However, in the case of overlapped EDL, the smoothly distributed electrical stress does not cause the contact angle change right at the triple contact line.

The above facts are fundamentally different from the macroscale problems and provide the motivations of the current research. In the present work, continuum analysis based on the electromechanical method is adopted to study the characteristics of electrocapillarity effect in the scale of $O(10 \text{ nm})$. (Extension to the electrowetting problem is straightforward, but for simplicity, it is not considered here.) The Poisson-Boltzmann equation is solved for the overlapped EDL, and the solution is used to estimate the electrocapillarity effect. As will be shown later, the electrocapillarity effect is represented by the sum of the osmotic pressure contribution and the Maxwell stress contribution. Then the deformed interface shape is also predicted by the first order domain perturbation technique. Although we are interested in both the nanotube and nanoslit problems, for simplicity, we consider only the two-dimensional problem of electrocapillarity effect in a nanoslit in the present work. In order to handle the problem analytically, two limiting situations are considered: (i) the low surface potential limit to have the linearized Poisson-Boltzmann equation [28,29], and (ii) the high surface potential limit for which it is assumed that only the counterions are present inside the nanoslit.

II. NORMAL STRESS EXERTED ON A SURFACE IN ELECTROLYTE

When there is no fluid flow and no gravity effect, the total stress can be described as the sum of the osmotic pressure contribution and the Maxwell stress contribution

$$\mathbf{T} = -\pi \mathbf{I} + \varepsilon \varepsilon_0 \left[\mathbf{E}\mathbf{E} - \frac{1}{2} E^2 \mathbf{I} \right], \quad \mathbf{E} = E(x) \mathbf{e}_x \quad (1)$$

where π is the osmotic pressure [31,32]. In the case of the nanoslit, we assume that the electric field has only the x component.

A. Normal stress exerted on a surface parallel to the slit axis

Let us first consider the normal stress exerted on the plane S_1 , which is a plane parallel to the slit axis, as shown in Fig. 1. Then T_{xx} is the inward x -directional normal stress exerted on the surface S_1 . The outward normal stress $-T_{xx}$ acts like the pressure but it is not isotropic. So, we denote it by

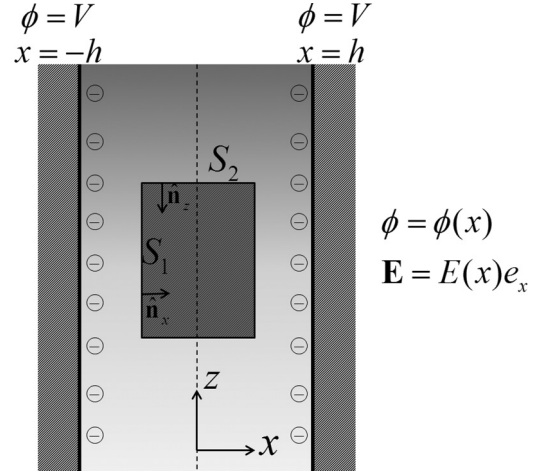


FIG. 1. The total normal stress (osmotic pressure contribution + Maxwell stress contribution) exerted on the plane parallel to the slit axis (S_1) and that exerted on the plane perpendicular to the slit axis (S_2).

P_{xx} and it is given as

$$-P_{xx} \equiv T_{xx} = -\pi(x) + \frac{\varepsilon \varepsilon_0}{2} E(x)^2. \quad (2)$$

In Eq. (2), the osmotic pressure can be obtained from the relation

$$\nabla \pi = \rho_f \mathbf{E} \quad \text{and} \quad \rho_f = \varepsilon \varepsilon_0 \nabla \cdot \mathbf{E}, \quad (3)$$

where ρ_f is the free charge density [16]. For the unidirectional electric field given in Eq. (1), we have

$$\pi(x) = \frac{\varepsilon \varepsilon_0}{2} E_x^2 + \text{const} = \frac{\varepsilon \varepsilon_0}{2} E^2 + \text{const} = \frac{\varepsilon \varepsilon_0}{2} E^2 + \pi(0). \quad (4)$$

At the centerline of the nanoslit, the electric field vanishes and we have Eq. (4). By substituting (4) into (2), we have a very important relation

$$-P_{xx} = T_{xx} = -\pi(0) = \text{const} \quad \text{with respect to } x. \quad (5)$$

The total outward normal stress on the plane S_1 is constant across the slit width and the value is the same as the osmotic pressure at the centerline. This is the well-known result which is available in a reference such as Israelachvili [33]. Further noteworthy works on the repulsive pressure along the same direction have been performed by Biesheuvel and other researchers [28,34–36]. They used the simplified versions of the Poisson-Boltzmann equation to obtain the formulas of the repulsive pressure for certain limiting situations.

B. On a surface perpendicular to the slit axis

In the case of a surface perpendicular to the slit axis such as S_2 in Fig. 1, we have the outward normal stress on S_2 as

$$-P_{zz} = T_{zz} = -\pi - \frac{\varepsilon \varepsilon_0}{2} E^2. \quad (6)$$

By comparing this equation with Eq. (2), we should note that there is a *sign change* in the Maxwell stress contribution. This makes the P_{ij} field anisotropic and the

outward normal stress exerted on the surface perpendicular to the slit axis is not uniform across the slit width. As will be shown later, this nonuniform distribution of P_{zz} causes the interface deformation. A similar lateral pressure concept has been adopted for the problem of microcantilever with polyelectrolyte brush [37] and the elastomer problem [38].

III. NORMAL STRESS EXERTED ON THE ELECTROLYTE-GAS INTERFACE UNDER THE CONSTANT SURFACE POTENTIAL CONDITION

Let us now consider the electrolyte-gas (or electrolyte-dielectric fluid) interface as shown in Fig. 2. We can consider any deformed interface in principle, but here we limit our attention only to the flat interface in order to treat the problem analytically. Here we further assume that the electric permittivity of the electrolyte is much larger than that of the gas (or dielectric fluid), i.e., $\epsilon \gg \epsilon_{out}$. Then the component of the electric field normal to the interface vanishes and the assumption that $\mathbf{E} = E\mathbf{e}_x = E(x)\mathbf{e}_x$ is still valid up to the electrolyte-gas interface. Since there is no osmotic pressure inside the gas phase and the electric permittivity of gas phase (or dielectric fluid phase) is much smaller than that of the electrolyte phase, the normal stress contribution inside the gas phase can be neglected compared to the electrolyte counterpart.

The outward normal stress on the electrolyte-gas interface P_{zz} results in the capillary rise in the gravity field as shown in Fig. 3(a). When the capillary rises, the inside pressure P_{in} is reduced. But P_{zz} compensates the reduction of the inside pressure and makes a balance to the outside pressure P_{out} . In the case of the closed slit as shown in Fig. 3(b), the electrolyte penetrates deeper into the slit until P_{out} is increased due to compression to make the balance with $P_{in} + P_{zz}$.

For computation of P_{zz} by Eq. (6), we need the electric field distribution across the slit and the osmotic pressure at the centerline. To do that, we need to solve the Poisson-Boltzmann (PB) equation for the nanoslit problem. However, as well known, the analytical solution is not available for the full nonlinear PB equation for the finite domain problem.

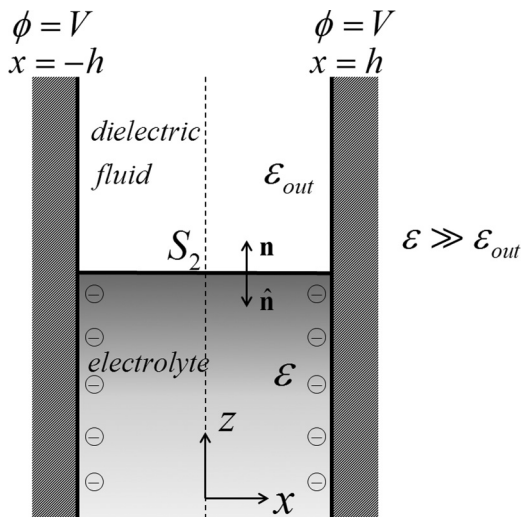


FIG. 2. The outward total normal stress exerted on the interface of electrolyte and dielectric fluid (e.g., gas).

Therefore, we consider two limiting cases, where analytic solutions are known for the approximate PB equations. They are (i) the low surface potential limit for which the linearized PB equation is solved, and (ii) the high potential limit for which it is assumed that coions are completely removed from the slit (i.e., only counterions are present inside the slit).

A. Low surface potential limit

We assume that one end of the nanoslit is connected to a large reservoir where both the positive and the negative ions have the same concentrations (the number density) n_b . In the case of low-voltage limit, i.e., $|ze\psi/kT| \ll 1$, we have the linearized Poisson-Boltzmann equation

$$\psi'' = \kappa^2 \psi, \quad \kappa^2 = \frac{2z^2 e^2 n_b}{\epsilon \epsilon_0 k T}, \quad (7)$$

where ψ is the electric potential, V is the surface electric potential at the electrode, and κ is the inverse of the Debye length.

The solution of (7) satisfying $\psi'(0) = 0$ and $\psi(h) = V$ is

$$\psi(x) = V \frac{\cosh \kappa x}{\cosh \kappa h} \quad (8)$$

and the x -directional electric field as

$$E_x = -\psi'(x) = -V\kappa \frac{\sinh \kappa x}{\cosh \kappa h}. \quad (9)$$

Therefore, the number density of ions along the slit centerline and the total number density are

$$\begin{aligned} n(0) &= 2n_b \cosh \left[\frac{zeV}{kT} \frac{1}{\cosh \kappa h} \right] \\ &\simeq 2n_b \left[1 + \frac{1}{2} \left(\frac{zeV}{kT} \right)^2 \left(\frac{1}{\cosh \kappa h} \right)^2 \right]. \end{aligned} \quad (10)$$

In the above, the low-voltage approximation has been adopted for the final step. Therefore the osmotic pressure along the centerline is

$$\pi(0) \simeq 2n_b kT + n_b kT \left(\frac{zeV}{kT} \right)^2 \frac{1}{(\cosh \kappa h)^2} \equiv \pi_b + \pi^e(0), \quad (11)$$

where π_b is the osmotic pressure in the bulk and $\pi^e(0)$ is the extra osmotic pressure due to the electric field effect. By substituting (9) and (11) into (6), we have the formula for the z -directional (outward) normal stress exerted on the electrolyte-gas interface due to electric field effect as

$$P_{zz}(x) = n_b kT \left(\frac{zeV}{kT} \right)^2 \frac{2 \cosh 2\kappa x}{\cosh 2\kappa h + 1} + 2n_b kT. \quad (12)$$

B. High surface potential limit

In the limit of high voltage V at the wall, the coions are excluded and the concentration becomes negligible inside the nanoslit. Thus, we may assume that only the counterions are present inside the nanoslit. With this approximation, we can obtain the analytical solution of the nonlinear Poisson-Boltzmann equation [33]. At the centerline of the nanoslit, the concentration of the counterions and the potential are denoted

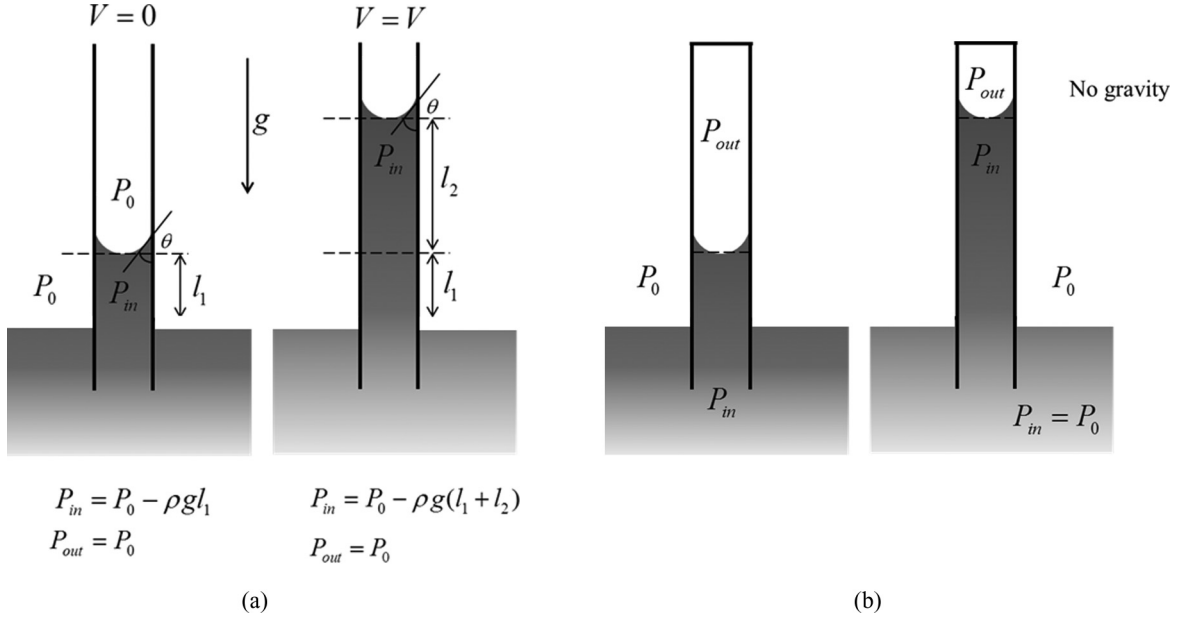


FIG. 3. The outward normal electrical stress P_{zz} results in the capillary rise in the gravity field [case (a)] or deeper penetration into a closed slit [case (b)].

by n_0 and ψ_0 . We have only negative ions in the slit if $V > 0$ and only positive ions in the case of $V < 0$. With the electric potential ψ_0 and the number density n_0 at the centerline, the governing equation and the boundary conditions are given as

$$\psi'' = \pm \left(\frac{ze n_0}{\epsilon \epsilon_0} \right) e^{\pm ze(\psi - \psi_0)/kT}, \quad \psi'(0) = 0, \quad \psi(h) = V, \quad (13)$$

where \pm denotes the positive V and negative potential, respectively. In this problem, we must note that the bulk concentration n_b and V may be specified. On the other hand, the values at the centerline of the nanoslit, n_0 and ψ_0 , must be determined as part of the solution.

The solution of (13) that satisfies the symmetry condition at the centerline is [33]

$$\psi(x) = V \pm \frac{2kT}{ze} \ln \left[\frac{\cos Kh}{\cos Kx} \right] \quad \text{with } K^2 = \frac{z^2 e^2 n_0}{2kT \epsilon \epsilon_0}. \quad (14)$$

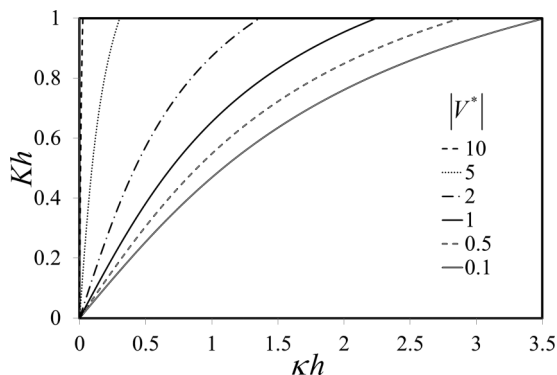


FIG. 4. Plot of Kh vs κh with the parameter $|V^*|$ [Eq. (16)].

The number density distribution $n(x)$ is obtained from (14) as

$$n(x) = n_0 e^{\pm ze(\psi - \psi_0)/kT} = \frac{n_0}{\cos^2 Kx} = \frac{n_b e^{ze|V|/kT} \cos^2 Kh}{\cos^2 Kx}. \quad (15)$$

In (15), the fact $n_0 = n_b \exp[ze\psi_0/kT]$ is used. By substituting the expression of n_0 in (15) into (14), we have

$$\frac{(Kh)^2}{\cos^2 Kh} = \frac{(\kappa h)^2}{4} e^{ze|V|/kT} \equiv \frac{(\kappa h)^2}{4} e^{|V^*|}, \quad (16)$$

where the dimensionless potential is scaled with the thermal voltage $V_{\text{therm}} = kT/ze$. For the given values of κh and V , we can compute the corresponding value of Kh by using (16). In Fig. 4, the plot of Kh vs κh is shown with $|V^*|$ as a dimensionless parameter.

The x -directional electric field is obtained from (14) as

$$E_x = -\psi' = \mp \sqrt{\frac{2kT n_0}{\epsilon \epsilon_0}} \frac{\sin Kx}{\cos Kx}. \quad (17)$$

On the other hand, the osmotic pressure inside the electrolyte is obtained from (15) as

$$\pi(x) = n(x)kT = n_0 kT \frac{1}{\cos^2 Kx}. \quad (18)$$

Therefore, the total outward normal stress is obtained from (6) as

$$P_{zz}(x) = \epsilon \epsilon_0 [E(x)]^2 + \pi(0) = n_0 kT (2 \tan^2 Kx + 1). \quad (19)$$

IV. NORMAL STRESS EXERTED ON THE ELECTROLYTE-GAS INTERFACE UNDER THE CONSTANT SURFACE CHARGE CONDITION

In many nanoslit or nanochannel systems, the wall condition may be characterized by the constant surface charge [39,40]. So, in this section, we want to transform the results of the previous section to the ones for the constant surface charge condition. For the analysis, we again consider two limiting cases of low surface charge limit and high surface charge limit.

A. Low surface charge limit

When we consider the case of constant wall charge with the surface charge density σ_w , we again assume that the potential is low, i.e., $|ze\psi/kT| \ll 1$. Then we have

$$\psi'' = \kappa^2 \psi, \quad \psi'(0) = 0, \quad \varepsilon \varepsilon_0 \psi'(h) = \sigma_w. \quad (20)$$

The solution of (20) is

$$\psi(x) = \left(\frac{\sigma_w}{\varepsilon \varepsilon_0 \kappa} \right) \frac{\cosh \kappa x}{\sinh \kappa h}. \quad (21)$$

By comparing (21) with (8), we can see that the potential distribution is the same as the case of constant voltage with

$$V = \frac{\sigma_w}{\varepsilon \varepsilon_0 \kappa} \left(\frac{\cosh \kappa h}{\sinh \kappa h} \right). \quad (22)$$

By substituting the above relation to the results in previous sections, we can derive the results for the case of constant surface charge. Specifically, we substitute (22) into (12) to have the expression of the average outward normal stress due to electric effect in terms of the surface charge.

$$\bar{P}_{zz}^e = \frac{\sigma_w^2}{4\varepsilon \varepsilon_0} \left(\frac{\sinh 2\kappa h}{(\sinh \kappa h)^2} \frac{1}{\kappa h} \right). \quad (23)$$

From (23), we can see that the normal stress is proportional to the square of the surface charge in the low surface charge limit.

B. High surface charge limit

In the case of constant wall surface charge density with σ_w , the governing equation and the boundary conditions are

$$\psi'' = \pm \left(\frac{ze n_0}{\varepsilon \varepsilon_0} \right) e^{\pm ze(\psi - \psi_0)/kT}, \quad \varepsilon \varepsilon_0 \psi'(h) = \sigma_w, \quad \psi'(0) = 0. \quad (24)$$

The solution of the governing equation with the boundary condition at $x = 0$ is given in (14). By using the solution, we apply the surface charge condition $[\varepsilon \varepsilon_0 \psi'(h) = \sigma_w]$ to have

$$\frac{2kT \varepsilon \varepsilon_0}{ze h} (Kh) \tan(Kh) = |\sigma_w|. \quad (25)$$

For the given surface charge, the intermediate parameter (Kh) is determined by solving Eq. (25). Then the extra outward normal stress can be computed by the previous Eq. (19), i.e.,

$$\bar{P}_{zz} = 2\varepsilon \varepsilon_0 \left(\frac{kT}{ze h} \right)^2 [2(Kh) \tan(Kh) - (Kh)^2]. \quad (26)$$

Equation (26) together with Eq. (25) is one of the major results in the present work. For the given surface charge, we can predict the average outward normal stress due to the electrocapillarity effect.

V. DEFORMATION OF THE ELECTROLYTE-GAS INTERFACE UNDER CONSTANT CONTACT ANGLE CONDITION

In this section, we are concerned with the interface deformation due to nonuniform outward normal stress [41]. Computation of the interface deformation starts with the normal stress condition [42] which includes surface tension.

$$\mathbf{n} \cdot (\mathbf{n} \cdot \mathbf{T}_{\text{out}}) - \mathbf{n} \cdot (\mathbf{n} \cdot \mathbf{T}_{\text{in}}) = \gamma \nabla \cdot \mathbf{n}, \quad (27)$$

$$\mathbf{T}_{\text{out}} = -P_{\text{out}}^h \mathbf{I}, \quad \mathbf{T}_{\text{in}} = -\pi \mathbf{I} + \mathbf{T}^e - P_{\text{in}}^h \mathbf{I}. \quad (28)$$

Here, the superscript h denotes the hydrostatic pressure and the surface tension γ is assumed to be constant for simplicity. (The surface tension is a function of the electrolyte concentration as shown by Onsager and Samaras [43], but the variation is relatively small compared to the value of pure water [43,44].) In order to treat the problem analytically, we use the domain perturbation technique and we introduce the shape function of the interface

$$F(x, z) = z - f(x) = 0. \quad (29)$$

Then we have the governing equation for the first order deformation as

$$f'' = -\frac{1}{\gamma} [P_{zz} - (P_{\text{out}}^h - P_{\text{in}}^h)] \equiv -\frac{1}{\gamma} [P_{zz} - \Delta P^h]. \quad (30)$$

A. Low surface potential limit

As mentioned earlier, for analytical treatment, we consider only the case of the initially flat interface. If the initial shape is not flat, we can handle the problem in the same way with the help of numerical computation of the stress field. The governing equation for the first order deformation is Eq. (30) and the boundary conditions are

$$f'(0) = 0, \quad f'(h) = 0 = \text{given value}. \quad (31)$$

The boundary condition at the wall ($x = h$) represents the assumption that the contact angle is not changed due to the change of ion concentration distribution. This assumption has been accepted for the electrowetting problem [11,16].

The unknown value of pressure difference $\Delta P^h \equiv (P_{\text{out}}^h - P_{\text{in}}^h)$ is determined to satisfy the condition of the given contact angle, i.e., $f'(h) = 0$ in Eq. (31). To derive the condition formally, we integrate (30) with the symmetry condition at $x = 0$ of (31) to have

$$\Delta P^h = (P_{\text{out}}^h - P_{\text{in}}^h) = \frac{1}{h} \int_0^h P_{zz} dx = \bar{P}_{zz}. \quad (32)$$

The result (32) tells us that we need to apply the required pressure difference that balances the average outward normal stress.

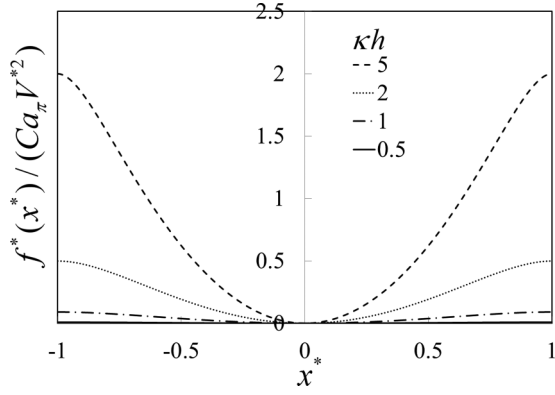


FIG. 5. Plot of $f^*/(\text{Ca}_\pi V^{*2})$ vs x^* with parameter κh . The interface is pushed outward more near the wall than the center [Eq. (34)].

The deformation of the interface using Eq. (30) satisfying the boundary conditions (31) is

$$\frac{f(x)}{h} = \frac{\varepsilon \varepsilon_0 (kT/zeV)^2 h}{4\gamma} \left(\frac{zeV}{kT} \right)^2 \times \frac{[-\cosh 2\kappa x + 1 + (\kappa x)(x/h) \sinh 2\kappa h]}{(\cosh 2\kappa h + 1)}. \quad (33)$$

We have $f(0) = 0$ and $f'(x) \geq 0$ for $0 \leq x \leq 1$ from (31). This means that electrical stress pushes out the interface more near the surface than near the center. The result (33) may be rearranged in a nondimensional form as

$$\frac{f^*(x^*)}{(\text{Ca}_\pi V^{*2})} = \frac{1}{2} \frac{[-\cosh[2(\kappa h)x^*] + 1 + (\kappa h)x^{*2} \sinh 2\kappa h]}{(\cosh 2\kappa h + 1)} \quad (34)$$

with

$$\text{Ca}_\pi = \frac{\varepsilon \varepsilon_0 (kT/zeV)^2 h}{2\gamma}, \quad (35)$$

where $x^* = x/h$ is the dimensionless coordinate, and $f^*(x^*) = f(x)/h$ is the dimensionless deformation. In (35), Ca_π is the capillary number based on the electric potential corresponding to thermal energy (thermal voltage) and V^* is the dimensionless voltage scaled with the thermal voltage as before. In Fig. 5, the plot of $f^*/(\text{Ca}_\pi V^{*2})$ vs x^* is given for several values of κh and we can see the effect of the increased bulk concentration by using the fact $\kappa \propto (n_b)^{1/2}$.

B. High surface potential limit

The deformation of interface under high surface potential limit is

$$f(x) = \frac{n_0 kT}{\gamma} \left[\frac{2}{K^2} \ln[\cos Kx] + \frac{\tan Kh}{Kh} x^2 \right] \quad (36)$$

or in dimensionless form with $f^* = f/h, x^* = x/h$,

$$f^*(x^*) = 4\text{Ca}_\pi \{ 2 \ln[\cos(Khx^*)] + (Kh) \tan(Kh)x^{*2} \}, \quad (37)$$

where the relationship between n_0 and n_b is used [Eq. (15)]. In Fig. 6, $f^*(x^*)/\text{Ca}_\pi$ vs x^* is shown with a parameter κh for a fixed value of $|V^*| = 0.5$. By comparing Figs. 5 and 6, we can

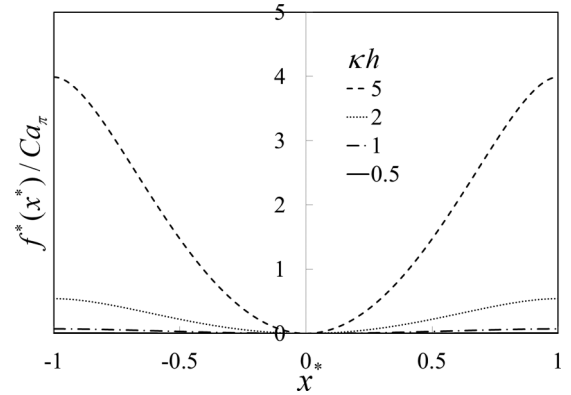


FIG. 6. Plot of $f^*(x^*)/\text{Ca}_\pi$ vs x^* with $V^* = 0.5$ and several values of κh [Eq. (37) together with Eq. (16) to compute Kh for the given κh and V^*].

see that the deformation behavior is very similar in both limits of the low and high surface potentials. However, the degree of deformation is much larger in the case of high potential limit. (By substituting $|V^*| = 0.5$ into Fig. 5, we can see how large the deformation is for the same surface potential.)

VI. DEFORMATION OF THE ELECTROLYTE-GAS INTERFACE UNDER FIXED CONTACT POINT

Now we consider the case of anchored contact points at $z = 0$, which cannot move. For this case, as before, we assume that the original interface shape is given by the balance between the osmotic pressure and the applied pressure, i.e.,

$$\Delta P_0^h = P_{\text{out}}^h - P_{\text{in}}^h = \pi_b = 2n_b kT. \quad (38)$$

In the previous case of constant contact angle, $\Delta P^h = P_{\text{out}}^h - P_{\text{in}}^h$ has to be changed to make a balance $\Delta P^h = \bar{P}_{zz}$. On the other hand, in this fixed contact point case, we do not have to change the pressure difference. Thus we just assume that $\Delta P^h = \Delta P_0^h = \pi_b$ even under the electric field effect and we have the governing equation and the boundary conditions for the shape function $f(x)$ as

$$f'' = -\frac{1}{\gamma} [P_{zz}(x) - \pi_b] = -\frac{1}{\gamma} P_{zz}^e(x) \quad (39)$$

with $f'(0) = 0$, $f(h) = 0$. The second boundary condition stands for the anchored contact point.

A. Low surface potential limit

Now let us consider the case of low surface potential. The shape function under this condition is

$$\frac{f(x)}{h} = \frac{1}{2} \frac{n_b kT h}{\gamma} \left(\frac{zeV}{kT} \right)^2 \left[\frac{\cosh 2\kappa h - \cosh 2\kappa x}{(\kappa h)^2 (\cosh 2\kappa h + 1)} \right]. \quad (40)$$

The solution in dimensionless form is

$$\frac{f^*(x^*)}{(\text{Ca}_\pi V^{*2})} = \frac{1}{2} \left[\frac{\cosh 2\kappa h - \cosh(2(\kappa h)x^*)}{(\cosh 2\kappa h + 1)} \right], \quad (41)$$

where $x^* = x/h$ is again the dimensionless coordinate, $f^*(x^*) = f(x)/h$ is the dimensionless deformation, and Ca_π is the thermal capillary number defined earlier below Eq. (35).

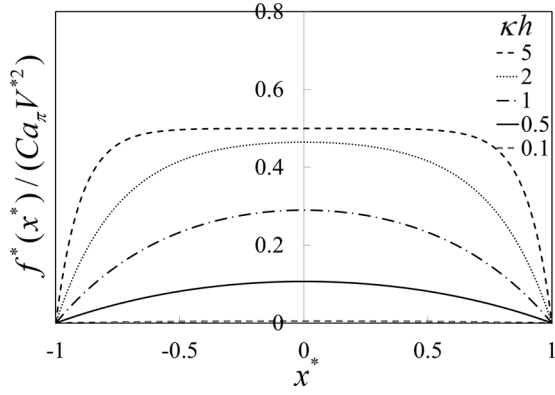


FIG. 7. Plot of $f^*/(Ca_\pi V^2)$ vs x^* in the case of fixed contact points for the low-voltage limit [Eq. (41)].

The result (41) is shown in Fig. 7, and we can see that a more convex interface shape is obtained as the electric effect is increased.

B. High surface potential limit

In the case of the high surface potential limit, the bulk phase osmotic pressure is negligible compared to the normal stress due to electric effect, i.e., $P_{zz}(x) \sim P_{zz}^e(x)$. Thus by substituting Eq. (19) into (39), we have the shape function as

$$f(x) = \frac{n_0 k T}{\gamma} \left[\frac{2}{K^2} \ln[\cos Kx] + \frac{1}{2}(x^2 - h^2) \right] \quad (42)$$

or in dimensionless form with $f^* = f/h$, $x^* = x/h$,

$$f^*(x^*) = 4Ca_\pi \left[2 \ln[\cos(Khx^*)] + \frac{(Kh)^2}{2}(x^{*2} - 1) \right]. \quad (43)$$

Here we should note once again that the parameters (κh) and $|V^*|$ can be specified. The parameter (Kh) must be determined according to Eq. (16). In Fig. 8, $f^*(x^*)/Ca_\pi$ vs x^* is shown with a parameter κh for a fixed value of $|V^*| = 0.5$.

VII. DISCUSSION

In the present work, the effect of EDL overlapping on the electrocapillarity effect inside a nanoslit has been analyzed.

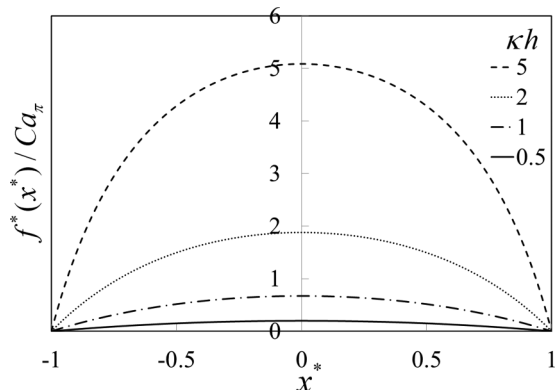


FIG. 8. Plot of f^*/Ca_π vs x^* for $|V^*| = 0.5$ in the case of fixed contact points for the high voltage limit [Eq. (43) with Eq. (16)].

For analytical treatment, we have considered an initially flat electrolyte-gas interface and two limiting situations of the low potential limit and the high potential limit. The results for the constant surface potential conditions are also transformed to the results for the constant surface charge conditions.

In the case of low potential limit, the z -directional outward normal stress is given by Eq. (12). Excluding the second term in Eq. (12), which is the osmotic pressure due to bulk concentration, the extra normal stress generated by the electrical effect has limiting forms. When $\kappa h \rightarrow 0$, the extra normal stress goes to $(n_b k T)(zeV/kT)^2$, and to $(n_b k T/\kappa h)(zeV/kT)^2$ when $\kappa h \rightarrow \infty$. On the other hand, in the case of high potential limit, we can predict the normal stress by Eq. (19) together with Eq. (16). The extra normal stress goes to $(n_b k T)e^{|zeV/kT|}$ when $\kappa h \rightarrow 0$, and to $[4(n_b k T)/\kappa h]e^{(1/2)|zeV/kT|}$ when $\kappa h \rightarrow \infty$.

Here it is noteworthy that $\bar{P}_{zz}^e \rightarrow P_{xx}^e = \pi^e(0)$ in the limit $\kappa h \rightarrow 0$. In other words, the axial directional (z -directional) outward normal stress approaches the value of repulsive pressure (which is the same as the osmotic pressure at the centerline). This is because the potential profile becomes flattened due to the fact that Debye length is much larger than the slit gap size. Indeed, the expression for the $\kappa h \rightarrow 0$ limit agrees with the expression of the repulsive pressure in Ref. [34] [his Eq. (20)]. However, it should be emphasized that $\bar{P}_{zz}^e > P_{xx}^e = \pi^e(0)$ except for that limit, i.e., the axial outward normal stress is larger than the repulsive pressure. Another thing we may note is the effect of bulk concentration [note that $\kappa \propto (n_b)^{1/2}$]. Under the constant surface potential condition, the extra normal stress is proportional to the bulk concentration of the electrolyte when the electrolyte is dilute ($\kappa h \rightarrow 0$), while it is proportional to the square root of bulk concentration for the high concentration case ($\kappa h \rightarrow \infty$).

Under the constant surface charge condition, the above results can be transformed to the ones shown below. First in the low surface charge limit, we have from Eq. (23). The extra normal stress goes to $(\sigma_w^2/2\epsilon\epsilon_0)[1/(\kappa h)^2]$ when $\kappa h \rightarrow 0$, and to $(\sigma_w^2/2\epsilon\epsilon_0)(1/\kappa h)$ when $\kappa h \rightarrow \infty$. For the high surface charge limit, from Eq. (26) together with Eq. (25) we have limiting forms. The extra normal stress goes to $(kT/zeh)|\sigma_w|$ when $|\sigma_w| \rightarrow 0$, and to $2(kT/zeh)|\sigma_w|$ when $|\sigma_w| \rightarrow \infty$. As in the case of constant potential, $\bar{P}_{zz}^e \rightarrow P_{xx}^e = \pi^e(0)$ in the limit $\kappa h \rightarrow 0$ (or $|\sigma_w^*| \rightarrow 0$). The expressions for the limiting cases agree with those for the repulsive pressure in Ref. [34] [his Eqs. (27) and (37)]. However, we must note once again that that $\bar{P}_{zz}^e > P_{xx}^e = \pi^e(0)$ except for that limit.

Under the dilute electrolyte condition ($c_{\text{bulk}} = 1 \text{ mM}$), the surface tension of water at room temperature ($\gamma = 71.97 \text{ mN/m}$) and the dielectric constant ($\epsilon_r = 80$) are used to estimate the deformation of shape function in dimensional form. In the low surface potential case [$V = 1 \text{ mV} \ll (kT/ze)$], the deformation is in the order of femtometers, which is hardly observable even in a nanochannel with a width of 50 nm. In the high potential case [$V = 1 \text{ V} \gg (kT/ze)$], however, the deformation is in the order of several nanometers and proportional to V^2 .

Thus far, no controlled experiment for the electrowetting or electrocapillarity effect has been performed for a nanoslit of $O(10 \text{ nm})$. So, direct comparison of the results of the present work with the experimental results is not possible. We have only the experimental results of related nanopore problems.

Kong and Qiao measured the extra pressure that is needed to be applied to the external fluid in order to make a balance to the electrocapillarity effect [24]. Their electrode had randomly generated nanopores of the average size $r = 480$ nm. Lu *et al.* also measured the needed extra pressure for the nanopores that are present in the confined region between the folded structures of an insulated electrode [25]. They observed qualitatively similar behaviors of the extra pressure. When the potential is small, the increasing rate of the extra pressure is small. On the other hand, for higher applied potential, the slope becomes much larger as we can see for the high potential limit. For the even higher potential values, they observed that the slope becomes small again. This saturation behavior has not been predicted by our current theoretical model. For this behavior, Lu *et al.* speculated that one possible reason is the steric effects of ions. In the nanopores, the sizes of ions cannot be totally neglected [45]. For the analysis of this behavior, previous works on the steric effects of ions may be consulted [16,46].

Another related problem is the electric-field-induced wetting and dewetting in a single hydrophobic nanopore [47]. When the hydrophobicity is not perfect, the electrolyte droplets can be trapped with the anchored boundary condition. If an electric field is applied in this situation, the droplets are extended in the electric field direction and they are connected to each other to make a path of electric current. That situation is very similar to the situation in Fig. 7 or 8, where the electrolyte-gas interface is elongated near the slit center.

VIII. CONCLUSIONS

We have analyzed the effect of EDL overlapping on the electrocapillarity in a nanoslit of $O(10$ nm) and have predicted the average outward normal stress generated by externally applied voltage or a given surface charge density. The normal stress in the direction parallel to the slit axis (the normal stress exerted on the surface perpendicular to the slit axis) is analytically studied under two limiting cases: low surface potential or charge case ($|ze\psi/kT| \ll 1$), and high surface potential or charge case ($|ze\psi/kT| \gg 1$). One of the important findings of the present work is that the total normal stress (osmotic pressure contribution + Maxwell stress contribution) is *not* isotropic. It is well known that the total normal stress in

the direction perpendicular to the slit axis is uniform across the slit width and the value is the same as the osmotic pressure at the centerline. On the other hand, it has not been well known that the total normal stress in the direction parallel to the slit axis is not the same as that in the perpendicular direction. Furthermore, the value of the normal stress in the parallel direction is not uniform across the slit width.

From the analysis, it is shown that the extra normal stress due to electrical effect is symmetric with respect to the sign of applied voltage as in the case of the macroscale electrowetting or electrocapillarity effect. In the low surface potential limit, the extra normal stress is proportional to the square of applied voltage. On the other hand, in the high potential limit, it increases exponentially with the magnitude of the applied voltage. In terms of surface charge, the normal stress is proportional to the square of the surface charge density in the limit of low surface charge. In the high surface charge limit, it is directly proportional to the magnitude of the surface charge density. Under the constant surface potential condition, the extra normal stress is proportional to the bulk concentration of the electrolyte when the electrolyte is dilute, while it is proportional to the square root of bulk concentration for the high concentration case.

Using the normal stress balance at the electrolyte-gas interface, the deformation of the interface shape is predicted under the fixed contact angle condition and under the fixed contact point condition. The deformation of the interface shape increases with increase of the dimensionless parameter κh , which is the ratio of the slit thickness to Debye length. This result has some significance in that we can predict the shape of the interface when the average extra outward normal stress is estimated for a nanoporous material.

Based on the current theoretical study, the electrocapillarity in a nanoslit of other novel materials such as ionic liquid can be analyzed (see [48] for the macroscale problem). Also, a theoretical model for the electrocapillarity of unsymmetrical electrolytes can be developed based on the works done by Onsager [49,50].

ACKNOWLEDGMENTS

This research was supported by Basic Science Research Program through the National Research Foundation of Korea (NRF) funded by the Ministry of Science, ICT and Future Planning (Grant No. NRF-2013R1A1A2011956).

-
- [1] F. Mugele and J. C. Baret, *J. Phys.: Condens. Matter* **17**, R705 (2005).
 - [2] M. G. Pollack, R. B. Fair, and A. D. Shenderov, *Appl. Phys. Lett.* **77**, 1725 (2000).
 - [3] M. G. Pollack, A. D. Shenderov, and R. B. Fair, *Lab Chip* **2**, 96 (2002).
 - [4] B. Verge and J. Peseux, *Eur. Phys. J. E* **3**, 159 (2000).
 - [5] M. Z. Bazant and T. M. Squires, *Phys. Rev. Lett.* **92**, 066101 (2004).
 - [6] P. Paik, V. K. Pamula, M. G. Pollack, and R. B. Fair, *Lab Chip* **3**, 28 (2003).
 - [7] A. R. Wheeler, *Science* **322**, 539 (2008).
 - [8] S. Berry, J. Kedzierski, and B. Abedian, *J. Colloid Interface Sci.* **303**, 517 (2006).
 - [9] T. Krupenkin and J. A. Taylor, *Nat. Commun.* **2**, 448 (2011).
 - [10] J. Newman and K. E. Thomas-Alyea, *Electrochemical Systems*, 3rd ed. (Wiley, New York, 2004).
 - [11] J. Buehrle, S. Herminghaus, and F. Mugele, *Phys. Rev. Lett.* **91**, 086101 (2003).
 - [12] P. M. Biesheuvel, *J. Colloid Interface Sci.* **275**, 514 (2004).
 - [13] T. B. Jones, *Langmuir* **18**, 4437 (2002).
 - [14] K. H. Kang, *Langmuir* **18**, 10318 (2002).

- [15] K. H. Kang, I. S. Kang, and C. M. Lee, *Langmuir* **19**, 5407 (2003).
- [16] C. K. Hua, I. S. Kang, K. H. Kang, and H. A. Stone, *Phys. Rev. E* **81**, 036314 (2010).
- [17] P. M. Biesheuvel and M. van Soestbergen, *J. Colloid Interface Sci.* **316**, 490 (2007).
- [18] T. B. Jones, J. D. Fowler, Y. S. Chang, and C. J. Kim, *Langmuir* **19**, 7646 (2003).
- [19] J. S. Hong, S. H. Ko, K. H. Kang, and I. S. Kang, *Microfluid. Nanofluid.* **5**, 263 (2008).
- [20] D. Mattia and Y. Gogotsi, *Microfluid. Nanofluid.* **5**, 289 (2008).
- [21] D. Bratko, C. D. Daub, K. Leung, and A. Luzar, *J. Am. Chem. Soc.* **129**, 2504 (2007).
- [22] S. Joseph and N. R. Aluru, *Nano Lett.* **8**, 452 (2008).
- [23] J. Y. Chen, A. Kutana, C. P. Collier, and K. P. Giapis, *Science* **310**, 1480 (2005).
- [24] X. Kong and Y. Qiao, *J. Appl. Phys.* **99**, 064313 (2006).
- [25] W. Lu, A. Han, T. Kim, V. K. Punyamurtula, X. Chen, and Y. Qiao, *Appl. Phys. Lett.* **94**, 023106 (2009).
- [26] P. M. Biesheuvel, S. Porada, M. Levi, and M. Z. Bazant, *J. Solid State Electrochem.* **18**, 1365 (2014).
- [27] S. Basu and M. M. Sharma, *J. Colloid Interface Sci.* **165**, 355 (1994).
- [28] J. E. Curry and D. A. McQuarrie, *J. Colloid Interface Sci.* **154**, 289 (1992).
- [29] S. L. Carnie and D. Y. C. Chan, *J. Colloid Interface Sci.* **161**, 260 (1993).
- [30] F. Mugele and J. Buehrle, *J. Phys.: Condens. Matter* **19**, 375112 (2007).
- [31] D. J. Griffiths, *Introduction to Electrodynamics*, 3rd ed. (Prentice Hall, Englewood Cliffs, NJ, 1999).
- [32] W. B. Russel, D. A. Saville, and W. R. Schowalter, *Colloidal Dispersions* (Cambridge University Press, Cambridge, UK, 1989).
- [33] J. Israelachvili, *Intermolecular and Surface Forces*, 2nd ed. (Academic, New York, 1992).
- [34] P. M. Biesheuvel, *J. Colloid Interface Sci.* **238**, 362 (2001).
- [35] D. Y. C. Chan, R. M. Pashley, and L. R. White, *J. Colloid Interface Sci.* **77**, 283 (1980).
- [36] K. Kohler, P. M. Biesheuvel, R. Weinkamer, H. Möhwald, and G. B. Sukhorukov, *Phys. Rev. Lett.* **97**, 188301 (2006).
- [37] F. Zhou, P. M. Biesheuvel, E. Y. Choi, W. Shu, R. Poetes, U. Steiner, and W. T. S. Huck, *Nano Lett.* **8**, 725 (2008).
- [38] R. Perline, R. Kornbluh, Q. Pei, and J. Joseph, *Science* **287**, 836 (2000).
- [39] B. V. Zhmud, A. Meurk, and L. Bergstrom, *J. Colloid Interface Sci.* **207**, 332 (1998).
- [40] H. Ohshima, *J. Colloid Interface Sci.* **212**, 130 (1999).
- [41] P. Kim, H. Y. Kim, J. K. Kim, G. Reiter, and K. Y. Suh, *Lab Chip* **9**, 3255 (2009).
- [42] L. G. Leal, *Advanced Transport Phenomena* (Cambridge University Press, Cambridge, UK, 2007).
- [43] L. Onsager and N. N. T. Samaras, *J. Chem. Phys.* **2**, 528 (1934).
- [44] Y. Levin and J. E. Flores-Mena, *Europhys. Lett.* **56**, 187 (2001).
- [45] W. Lu, T. Kim, A. Han, X. Chen, and Y. Qiao, *Langmuir* **25**, 9463 (2009).
- [46] S. Das and S. Chakraborty, *Phys. Rev. E* **84**, 012501 (2011).
- [47] M. R. Powell, L. Cleary, M. Davenport, K. J. Shea, and Z. S. Siwy, *Nat. Nanotechnol.* **6**, 798 (2011).
- [48] X. Hu, S. Zhang, C. Qu, Q. Zhang, L. Lu, X. Ma, X. Zhang, and Y. Deng, *J. Adhes. Sci. Technol.* **26**, 2069 (2012).
- [49] L. Onsager, *J. Am. Chem. Soc.* **86**, 3421 (1964).
- [50] R. M. Fuoss and L. Onsager, *J. Phys. Chem.* **68**, 1 (1964).